



## RESEARCH ARTICLE - ENGINEERING

## Friction Spot Joining of Aluminium Alloy AA 5052 to Pre-Holed Steel AISI 1006 by Extrusion of Aluminium into a Rivet Head Die

Isam Tareq Abdullah<sup>1\*</sup><sup>1</sup> Engineering Technical College -Baghdad, Middle Technical University, Baghdad, Iraq.\* Corresponding author E-mail: [isamtareq@yahoo.com](mailto:isamtareq@yahoo.com)

Article Info.	Abstract
<p><i>Article history:</i></p> <p>Received 01 March 2022</p> <p>Accepted 23 April 2022</p> <p>Publishing 30 June 2022</p>	<p>This work aims to join an aluminium alloy together with a pre-holed carbon steel sheet by extrusion the aluminium through a steel hole with a rivet shape to avoid the joint pull out. AA 5052 and AISI 1006 sheets were assembled with a lap structure such that the aluminium sample was placed above the steel. A rivet head die was put under the steel hole. The aluminium was extruded through the rivet head die passing via the steel hole utilizing a friction spot technique by a rotating tool. The influence of the hole diameter, rotating speed, and plunging depth of the tool on the rivet head dimensions and joints shear force and strength were investigated by the design of experiments approach. Joint macrostructure was examined. The aluminium metal was successfully extruded with a rivet shape. The steel hole diameter displayed the most increased influence on the rivet head dimensions and the joints' shear force. Incrementing the plunging depth of the tool raised the joint's shear strength. The joined samples failed by shearing the extruded aluminium at the steel hole surface without pull-out the formed rivet head. The joining mechanism appeared with a mechanical interlock and without the formation of inter-metallic compounds between the two materials. For the first time, the AA 5052 and pre-holed AISI 1006 sheets were joined by extrusion of the aluminium during a solid rivet head. The highest shear strength of the joint exceeded those of the AA 5052 by 55%.</p>
<p>This is an open-access article under the CC BY 4.0 license (<a href="http://creativecommons.org/licenses/by/4.0/">http://creativecommons.org/licenses/by/4.0/</a>)</p>	
<p>Publisher: Middle Technical University</p>	
<p><b>Keywords:</b> Friction Spot Joining; AA 5052; AISI 1006; Extrusion.</p>	

### 1. Introduction

A decrease in weight, fuel consumption, and toxic emissions attract attention in industrial applications. Most of the steel parts in various automotive, ships, aerospace, and industrial applications were replaced by aluminium alloys to decrease the overall weight of structures and fuel consumption [1]. Aluminium alloy AA 5052 is a non-heat treatable alloy and has good corrosion resistance, excellent mechanical characteristics, and high fatigue strength. Therefore, this type of aluminium alloy is commonly used in marine components, boats, and oil and fuel tubing. In various industrial applications, the aluminium alloys are welded or joined using different techniques [2].

Recently, friction stir welding (FSW) and friction spot stir welding (FSSW) techniques have been widely utilized in the welding of different materials such as steel and aluminium. These techniques are solid-state methods, which involve the formation of intermetallic compounds (IMCs) at an interface line between welded materials [3]. The IMCs types influence the welded quality and depend on the welded materials types and welding parameters [4]. Pourali et al., 2017 examined the IMCs formation in welding of St37 steel and AA1100. The joint's interface line contained two types of IMCs; FeAl and Fe<sub>3</sub>Al, with a thickness range of 4-93µm, depending on the welding parameters [5]. Chen et al., 2017 refilled the keyhole in the FSSW of AA6061 with high-strength steel. The hook structure contained thin layers of the IMCs [6]. Hsieh et al., 2017 observed two types of IMCs in FSS fusion welding of AA6061 to low carbon steel; Fe<sub>4</sub>Al<sub>13</sub> and Fe<sub>2</sub>Al<sub>5</sub>, with a thickness range of 1.5-25µm [7]. Helal et al., 2019 studied the influence of welding speed on the thickness of the IMCs in welding AA6061 to ultra-low carbon steel sheets. They found that the increment in the welding speed minimized the thickness of the IMCs, which increased the joint strength [8]. Jamshidi aval and Loureiro, 2019 enhanced the joint quality of AISI304 to AA7075 using the dual rotation FSW (DR-FSW) process. This process reduced the amount of IMCs formation compared to conventional FSW [9]. Wang et al., 2019 used a scribe tool in welding AA6022 to DP600 steel, which reduced the IMCs layer thickness to a Nano-scale [10]. Anaman et al., 2019 noticed the formation of IMC of FeAl in the stirred zone of AA5052-H32 to dual-phase steel joint [11]. Shen et al., 2019 noticed that the IMCs formation reduces the joint strength of AA5754 to coated steel.

Nomenclature			
AA	Aluminium Alloy	AISI	American Iron and Steel Institute
FSW	Friction Stir Welding	FSSW	Friction Spot Stir Welding
IMCs	Intermetallic Compounds	SPR	Self-Piercing Rivet
RSW	Resistance Spot Welding	FSE	Friction Stir Extrusion
DOE	Design of the Experiments	mm	Millimetre

The aluminium alloys have been joined to steel using different techniques to avoid the IMCs formation [12]. Cai et al., 2005 compared the joint properties using two methods; self-piercing rivet (SPR) and resistance spot welding (RSW). The results indicated that the SPR exhibited a higher joint distortion compared to that of the RSW [13]. Abe et al., 2006 examined the joining properties of AA5052 with mild steel using the SPR method. It was observed that penetrating the material determines defects of the joint [14]. Abe et al., 2009 joined AA5052 together with different types of high-strength steel using the SPR method. The joint's tensile strength reached a value of about 590MPa [15]. Lazarevic et al., 2013 joined AA6014 to AISI5182 using friction stir forming techniques. The joining mechanism appeared with a mechanical interlock between the two materials. The joints failed by two types of fracture modes: braze fracture and peeling the aluminium sheet [16]. Evans et al., 2015 used a friction stir extrusion (FSE) technique to join AA601 with low carbon steel. This method eliminated the formation of IMCs and joined the two materials with a mechanical interlock mechanism [17]. Huang et al., 2016 joined QSTE340TM steel with AA6082 using the self-riveting friction technique, in which the aluminium metal extruded through pre-holed steel holes. An average fracture load of the joints reached a value of 3.21kN. A metallurgical bonding occurred between the two materials with diffusion layers [18]. Huang et al., 2019 examined the self-riveting friction stir lap technique in joining AA6082 to QSTE340TM steel by filling pre-holes of the steel sheet with the formed aluminium during the process. The joint strength of the samples was raised by 23% compared to those of the FSW method [19]. Hussein et al., 2019 used a frictional forming technique to join AA5052 together with pre-holed and threaded AISI1006 steel by extruding the aluminium during the steel hole. The plunging depth of the tool displayed an increased influence on the joint strength [20]. In the previous studies, the joints may fail by shearing or pulling out the joined material. However, few studies have focused on preventing the joint pull-out. This study introduces a new design of joined specimens to avoid the pull-out. A friction spot (FS) method was utilized to join an aluminium alloy together with steel. The aluminium extruded through pre-holed steel with a rivet shape, with the aid of a rivet head die. Design of the experimental process (DOE) was utilized to design the experiments and analyse the influence of joining parameters on the joint properties. The Joint's macrostructure was investigated.

## 2. Experiments

### 2.1. Materials

AISI 1006 carbon steel and AA 5052 aluminium alloy sheets were selected to prepare specimens with a thickness of 1.5 & 2.4 mm, respectively. Table 1 lists the mechanical properties of each material [21].

Table 1 Mechanical properties of the AISI 1006 and AA 5052

Material	Tensile Strength (MPa)	Yield Strength (MPa)	Shear Strength (MPa)
AA 5052	195	90	125
AISI 1006	330	280	230

The specimens were manufactured with a width and length of 25 and 100 mm, respectively. A hole was machined in the steel specimen at the centre of the lap joint area, as exhibited in Fig. 1.

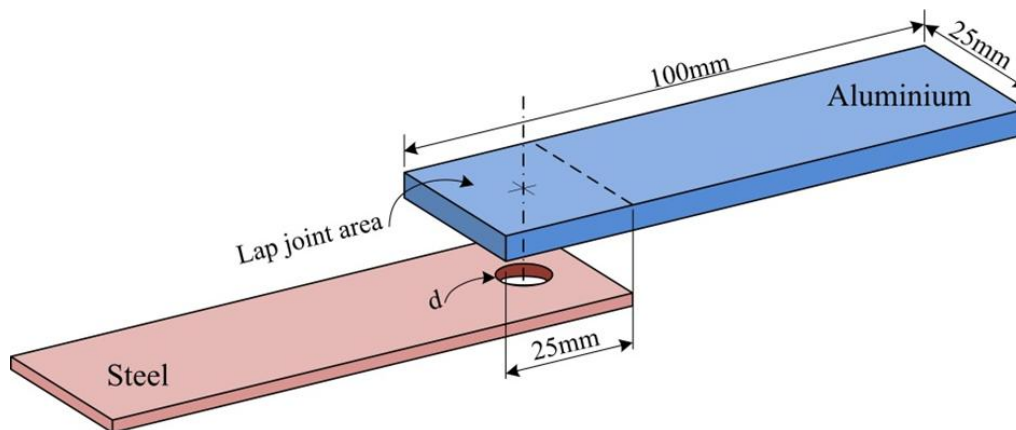


Fig 1. Specimen's dimensions

2.2. Lap joint configuration

Assembling of the specimen joint consisted of five steps as follows: putting a cylindrical die over a lower machine fixture, the steel specimen over the die, the aluminium specimen over the steel, and a collar over the aluminium specimen. Finally, an upper fixture was tightened with the machine base, with the aid of suitable bolts, as shown in Fig. 2. The die and collar were made from carbon steel material. The collar contains a hole of 11 mm in diameter. The die was drilled with a hole of 6 mm diameter and 1 mm depth. The rotating tool was manufactured from a carbide material with a diameter of 10 mm.

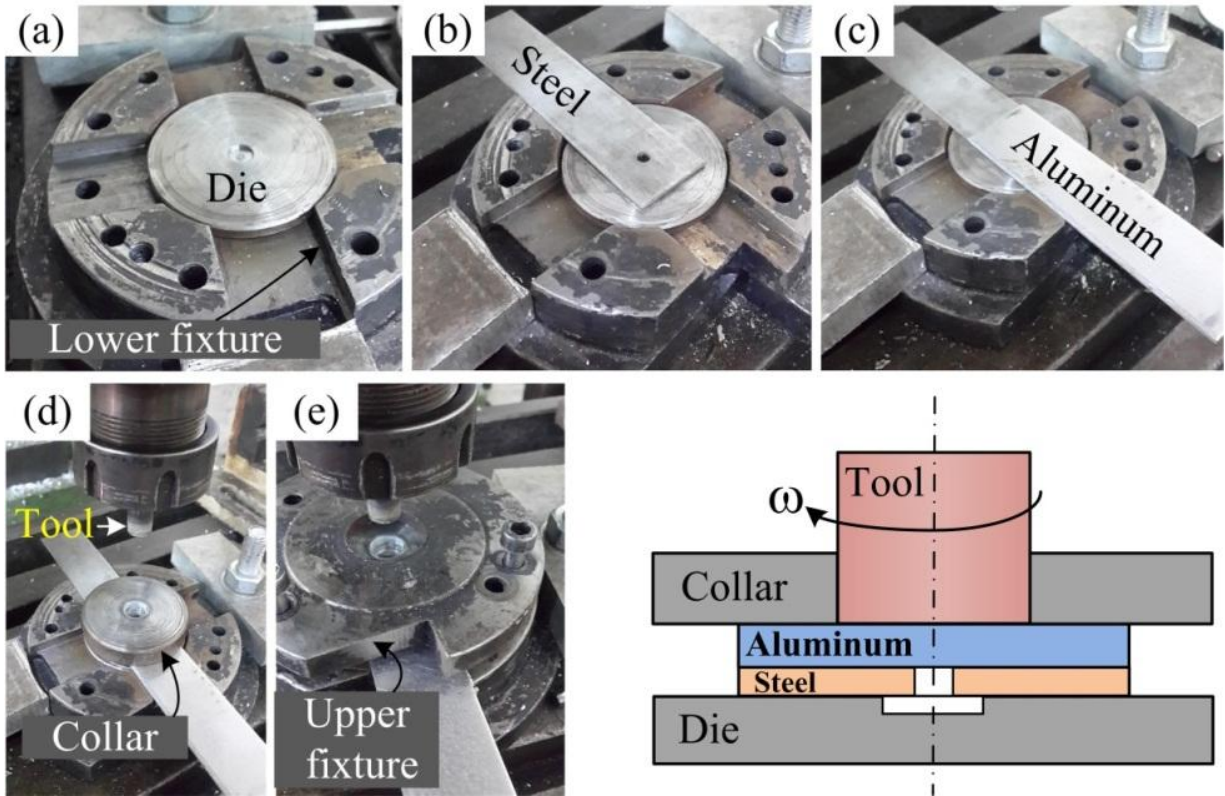


Fig 2. Lap joint assembly steps

2.3. Lap joint configuration

The joining technique was carried out in two steps: pre-heating the aluminium specimen by the rotating tool and plunging the tool into this specimen, as displayed in Fig. 3. Initially, the rotating tool touches the upper surface of the aluminium sample, as shown in Fig. 3a. The temperature increases gradually with time under the effect of the rotating friction between the tool and the aluminium specimen. The heat input softens the aluminium metal under the tool surface. In the second step, Fig. 3b, the pressure is applied to the rotating tool to plunge it through the softened aluminium. The soft aluminium flows and extrudes through the die hole passing through the steel hole and forming a rivet head shape. The function of the collar is to avert the formation of aluminium flash during the process. Finally, the rotating tool is removed upward; the final profile of the joint is shown in Fig. 3c. Dimensions of the formed rivet head were assumed as a diameter ( $D$ ) and a thickness ( $t$ ).

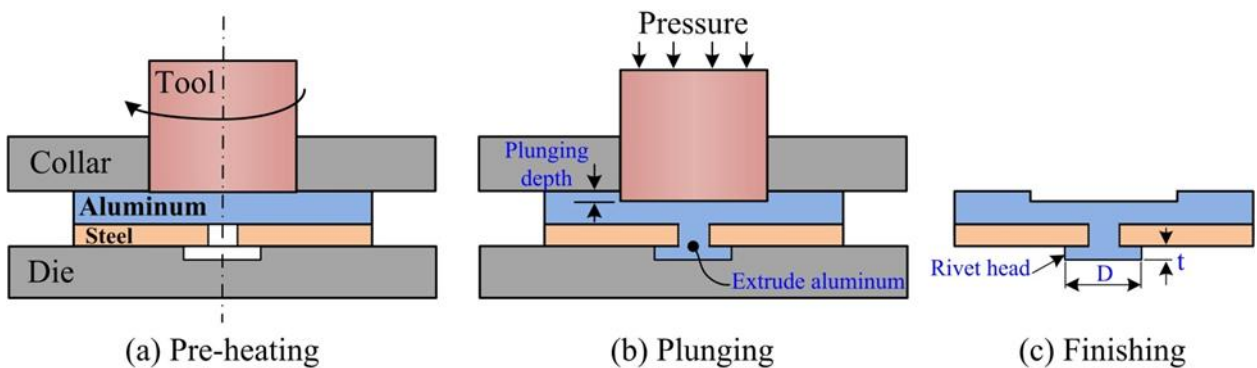


Fig 3. Schematic of the joining steps

#### 2.4. The process parameters and tests

The effect of three parameters on joining quality was studied; steel hole diameter, “rotating speed, and plunging depth of the tool”. Three estimates were examined for every parameter. The DOE approach was employed to design the experiments by the Taguchi method, with the assistance of the MINITAB program. Accordingly, nine experiments were designed with different parameters values to examine the joint quality between the two materials, as recorded in Table 2. The joining method of the specimens was carried out within a constant pre-heating time of 10 seconds. Fig. 4 illustrates a sample of the joined steel together with the aluminium. The joined samples were examined by the tensile, macrostructure, and X-ray diffraction (XRD) examinations.

Table 2 Taguchi's design of the process parameters

No.	Rotating Speed (RPM)	Plunging depth (mm)	Hole diameter (mm)
1	1120	0.5	2
2	1400	1.0	2
3	1800	1.5	2
4	1120	1.0	3
5	1400	1.5	3
6	1800	0.5	3
7	1120	1.5	4
8	1400	0.5	4
9	1800	1.0	4

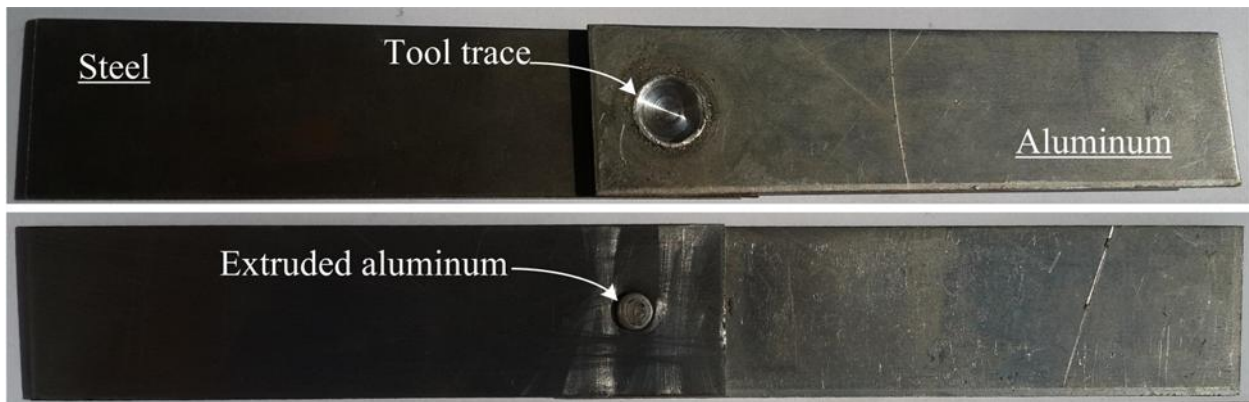


Fig 4. The joined sample

### 3. Results and Discussion

#### 3.1. Dimensions of rivet's head

The samples were joined with different rivet head dimensions (thickness and diameter). Fig. 5 displays the variation of the rivet head dimensions of the samples. Values of the rivet head diameter ranged from 2.32 to 5.30 mm, while the thickness ranged from 0.32 to 0.98 mm. The results indicated that the dimensions variation of the thickness and diameter exhibited the same behaviour for each sample. The dimensions increased gradually in samples No.1 to 5. Minimum and maximum rivet head dimensions were found in samples No.1 and 7, respectively. Both samples were joined with a minimum rotating speed;  $N=1120$  RPM. Sample No.1 was joined with minimum plunging depth and steel hole diameter, while sample No.7 was joined with maximum plunging depth and steel hole diameter, as indicated in Table II. Regardless of the rotating speed, it is evident that the highest plunging depth and steel hole diameter gave the maximum rivet head dimensions. The highest plunging depth of the tool occurs at maximum applied pressure, which raised the amount of the extruded aluminium during the steel hole and the rivet hole dimensions [20]. Moreover, incrementing the hole diameter of the steel sample raises the amount of extruded aluminium compared to the small diameter. Consequently, sample No.7 exhibited the largest rivet head dimensions compared with the other samples.

The rivet head dimensions were analysed by the DOE, as displayed in Fig. 6 and 7. The main effect plots show that the rivet head dimensions incremented with increasing the steel hole diameter and plunging depth of the tool. The line slope of the hole diameter plot is more than that of the plunging depth plot; this means that the increase in steel hole diameter increased the rivet head dimensions more than that of the plunging depth. The rotating speed had a small effect on the rivet head dimensions, which increased and decreased slowly at the rotating speed range of 1120 to 1400RPM and 1400 to 1800RPM. On the other hand, the Pareto chart demonstrates that the steel hole diameter displayed the maximum influence on the rivet head dimensions followed by the plunging depth and rotating speed.

The rivet head diameter and thickness formulas were estimated from the DOE analysis as functions of the experimental parameters, Table 3 lists the coefficients formulas. The rivet head dimensions were experimentally measured and plotted together with the predicted formulas, as shown in Fig. 8. The calculated dimensions from the predicted formulas exhibited a good agreement with the experimentally measured.

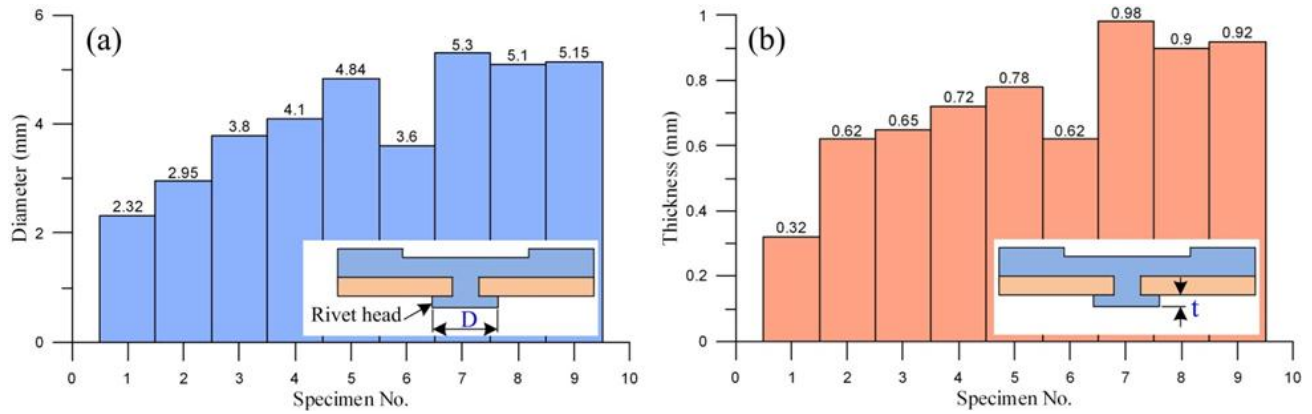


Fig 5. Rivet's head dimensions for each sample; (a) diameter, (b) thickness

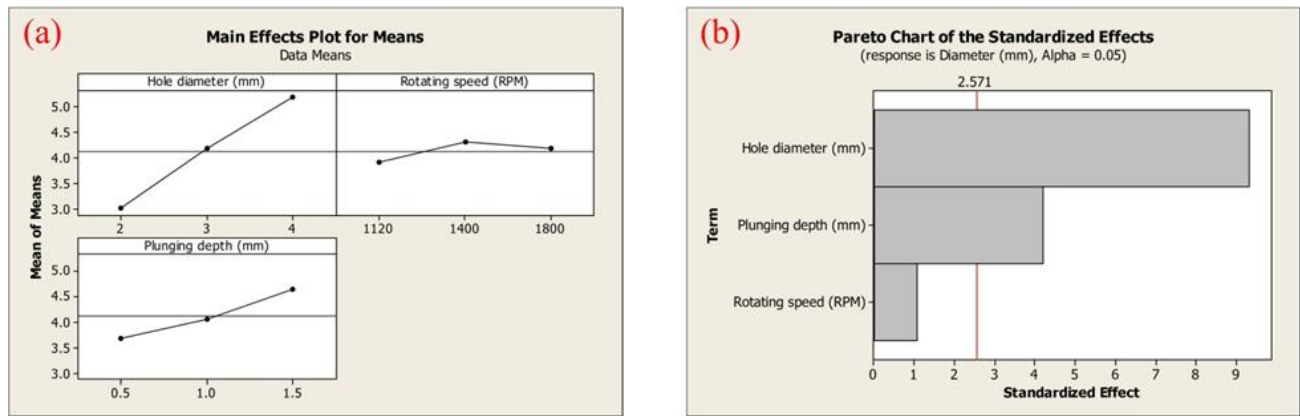


Fig 6. DOE analysis of rivet head diameter; (a) main effect plot, (b) Pareto chart

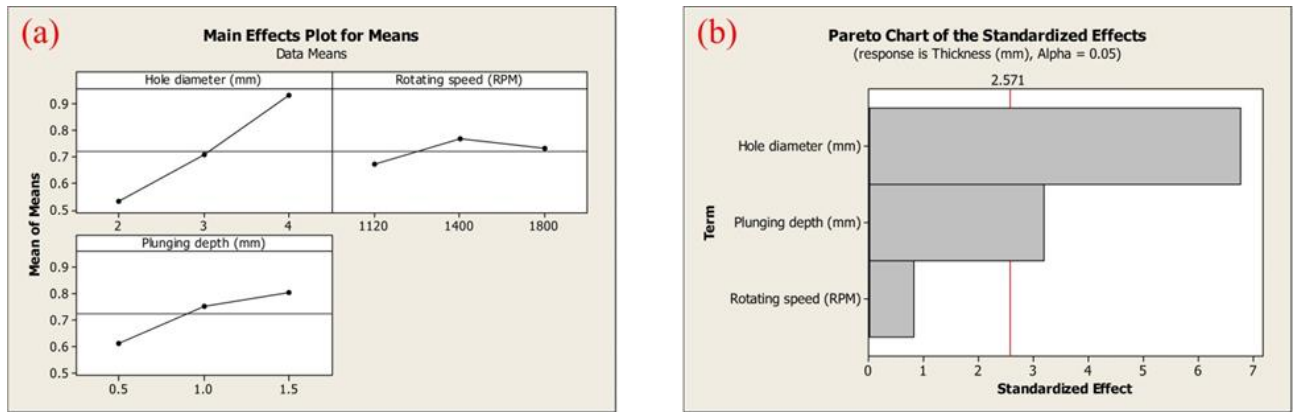


Fig 7. DOE analysis of rivet head thickness; (a) main effect plot, (b) Pareto chart

Table 3 Functions coefficients of rivet hole diameter and thickness

Term	Hole diameter coefficients	Thickness coefficients
Constant	-0.6022	-0.1744
Hole diameter (mm)	1.08	0.20167
Rotating speed (RPM)	0.00036	$7.135 \times 10^{-5}$
Plunging depth (mm)	0.9734	0.19

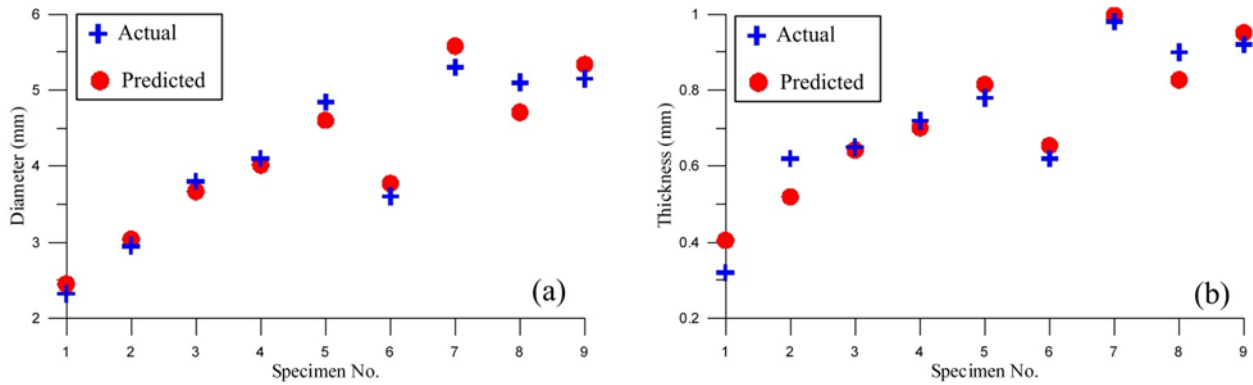


Fig 8. The experimental and predicted rivet head dimensions; (a) diameter, (b) thickness

### 3.2. Shear test of the samples

The joined samples were tested by the tensile test. All the specimens failed by shearing the extruded aluminium, without pulling out the joint. The fracture force was recorded and considered as a shear force of the joined region. Fig. 9a displays the recorded shear forces of the joints. The samples can be divided according to the steel hole diameter (d) as follows: set 1 of d= 2 mm (samples No. 1, 2, and 3), set 2 of d= 3 mm (samples No. 4, 5, and 6) and set 3 of d= 4mm (samples No. 7, 8 and 9). According to the samples sets sequence, the shear force increased with increasing the steel hole diameter. Samples No. 3 and 8 exhibited the minimum and maximum shear force values, respectively. Increasing the hole diameter allows for passing a higher amount of the extruded aluminium during the joining process compared with the small diameter. The higher amount of the extruded aluminium through the steel hole increased the joined region and the rivet head dimensions, which decreases the ability to pull out the extruded aluminium from the steel specimen [22]. So, the sample of maximum hole diameter (No. 8) exhibited the highest value of the shear force. The shear force values of the samples in each set were convergent.

The shear strength of the samples was calculated at the fractured region of the extruded aluminium, as shown in Fig. 9b. Shear strength values of the samples ranged between 149 and 194 MPa. The shear strength of samples exceeded those of the wrought aluminium alloy AA5052; this means that the mechanical properties of the extruded aluminium slightly improved. During the frictional joining process, the aluminium is extruded with a higher temperature and heat treatment effect, which improves the mechanical properties [23].

On the other hand, the experimental data of the tensile test were analysed using the DOE method. Fig. 10 displays the DOE analysis of the joint's shear forces. The main effect plot indicates that the joint's shear force increases with increasing the steel hole diameter. The joint's shear force was insignificantly affected by the rotating speed and plunging depth of the tool. The Pareto plot indicates that the steel hole diameter has the highest effect on the joint's shear force compared with the other parameters.

The shear strength of the joints was analysed by the DOE, as shown in Fig. 11. The plunging depth of the tool has a higher effect on the mechanical properties of the joints [24]. The main effect plot indicates that the shear strength decreases with increasing the plunging depth. Moreover, the Pareto chart indicates that the plunging depth has the most effect on the joint's shear strength compared to the other parameters.

The shear force and strength formulas of the joints were estimated in terms of the experimental parameters according to the DOE analysis, as illustrated in Table 4. Fig. 12 shows the predicted formulas and the recorded shear force and strength. The predicted shear force formula exhibited a good agreement with the experimental shear forces data. Approximately, the predicted formula of the shear strength agreed with five samples.

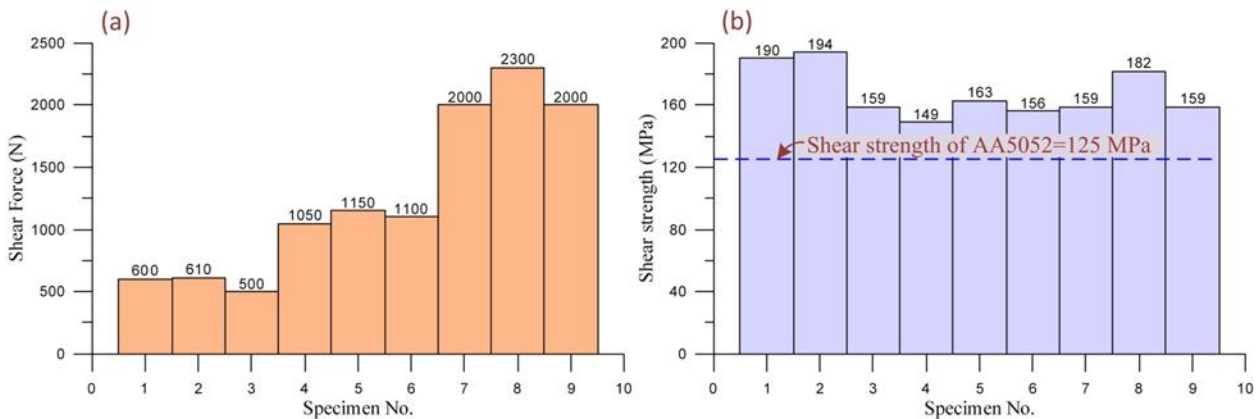


Fig 9. Shear tests of the samples; (a) shear force, (b) shear strength

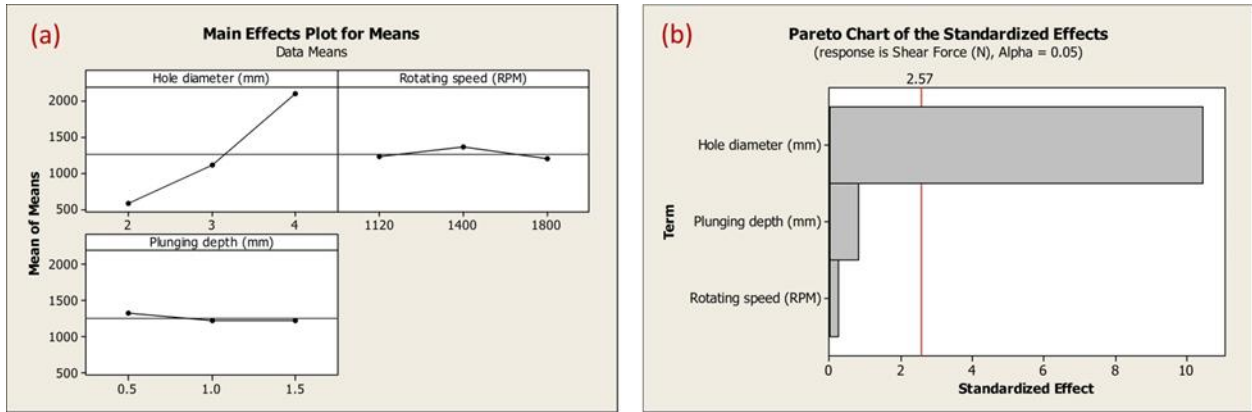


Fig 10. DOE analysis of joints shear force; (a) main effect plot, (b) Pareto chart

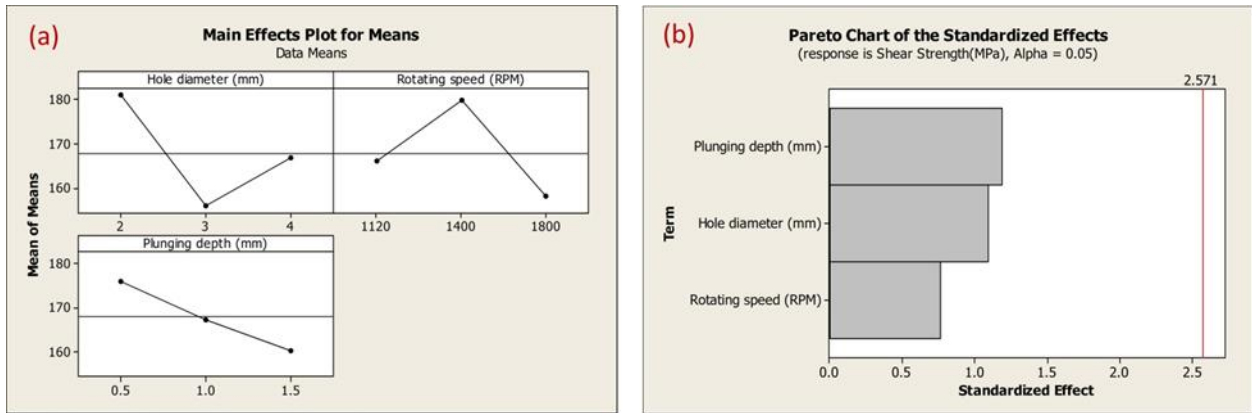


Fig 11. DOE analysis of joints shear strength, (a) main effect plot, (b) Pareto chart

Table 4 Coefficients of shear force and strength functions

Term	shear force coefficients	shear strength coefficients
Constant	-851	226.2
Hole diameter (mm)	765	-7.17
Rotating speed (RPM)	-0.05	-0.015
Plunging depth (mm)	-116.7	-15.7

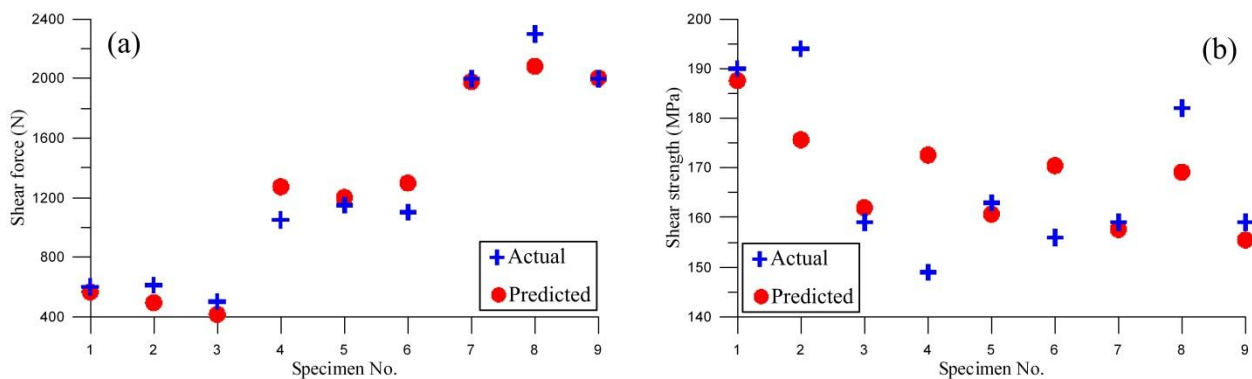


Fig 12. The experimental and predicted data, (a) shear force, (b) shear strength

### 3.3. Joined and fractured surface features

Fig. 13 shows images of the outer and fracture surfaces of the samples. The upper surfaces of the aluminium specimens indicated that the collar prevented the formation of aluminium flash compared with the conventional FSSW [25]. Reducing the flash formation during the friction spot mechanism reduced aluminium losses. The rivet head images indicate that the aluminium metal extruded successfully through

the steel hole and formed the rivet head shape with the aid of the die. The samples exhibited a different amount of extruded aluminium depending on the joining conditions. In the samples with a higher amount of extruded aluminium, the aluminium metal touched the die surface and formed a die trace, as clearly observed in samples No. 4, 5, 6, 7, and 9. The fracture surfaces indicated that the tested samples failed by shearing the extruded aluminium without pulling out the rivet head. Approximately, for all the samples, the extruded aluminium filled the steel hole.













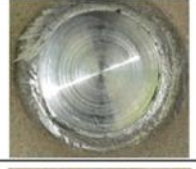















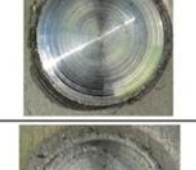







No.	Joined surfaces		Fractured surfaces	
	Upper surface of Aluminum	Rivet head	Fractured surface of Aluminum	Inner surface of Steel
1				
2				
3				
4				
5				
6				
7				
8				
9				

Fig 13. Joined and fractured surfaces of the samples



### 3.4. Joined macrostructure

Sample No.8, of the maximum shear force, was selected to examine the macrostructure features of the joint cross-section, as shown in Fig. 14. The aluminium specimen surface, near the tool trace, is plastically deformed due to the higher applied pressure and input heat during the joining process [3]. The heat-affected zone (HAZ) appears in the aluminium specimen with an asymmetrical shape. The HAZ started from the upper surface of the aluminium surface and expanded along with the thickness of the aluminium specimen. The extruded aluminium filled the steel hole without gaps.

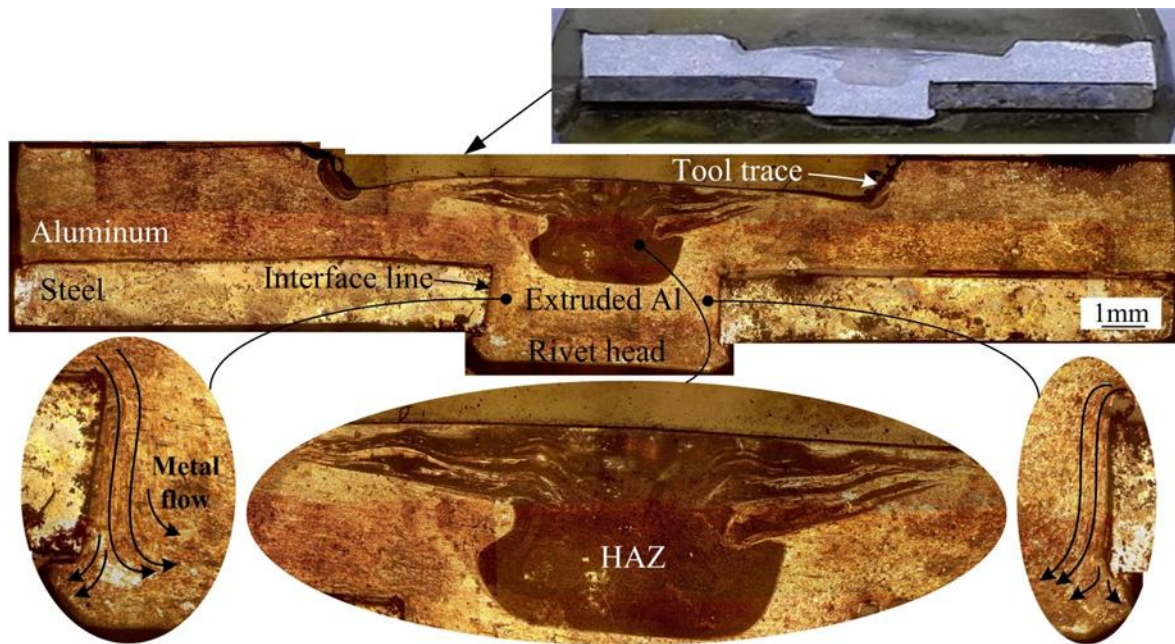


Fig 14. Macrostructure of joint cross-section, sample 8

### 3.5. X-ray diffraction (XRD) joint test

The formation of IMCs at the interface line between the extruded aluminium and the inner surface of the steel hole was examined by the XRD test, as shown in Fig. 15. The XRD analysis demonstrates that the joining mechanism occurred without the IMCs formation between the two materials. The recorded peaks reveal that the interface line consisted of two types of chemical elements; Al and Fe, which represent the joined materials. Moreover, the peaks revealed that the joining at the interface line occurred without phases or IMCs formation. Accordingly, the joining mechanism occurred by mechanical interlock between the AA5052 and AISI1006 [20].

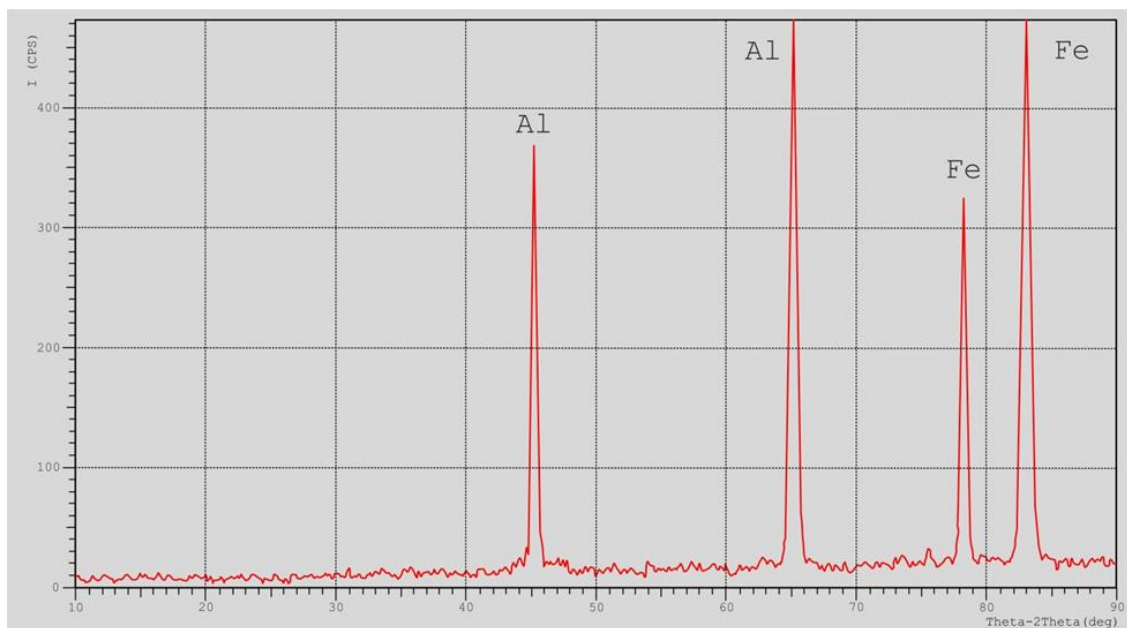


Fig 15. XRD plot of the joint interface, sample 8

#### 4. Conclusion

AA5052 was joined together with a pre-holed AISI1006 by extruding the aluminium through the steel hole with a rivet head end using the FS method. The following conclusions were drawn:

- 1- The two materials were joined by a mechanical interlock mechanism without the formation of IMCs or metal loss.
- 2- Increasing the hole diameter of the steel specimen and plunging depth of the tool increased the rivet head dimensions, which increased the joint's shear force.
- 3- The rivet head thickness and diameter reached a maximum value of 0.98 and 5.3mm, respectively.
- 4- The steel hole diameter exhibited the highest effect on the rivet head dimensions followed by the plunging depth and the rotating speed of the tool.
- 5- The joint's shear strength reached a maximum value of 194 MPa, which exceeded that of the AA5052 by 55%.
- 6- Increasing the plunging depth of the tool reduced the joints' shear strength.
- 7- The tool plunging depth exhibited the highest effect on the joint's shear strength, followed by the steel hole diameter and the rotating speed of the tool.
- 8- All the tested samples failed by shearing the extruded aluminium without pulling out the formed rivet head.
- 9- The predicted formulas for the rivet head dimensions and shear force and strength of the joints exhibited good agreement with the experimental data.

#### Acknowledgement

We would like to thank to head of the applied mechanical Engineering department and all teaching staff of the department for their assistance.

#### Reference

- [1] Watanabe, T., Takayama, H. and Yanagisawa, A. (2006), "Joining of aluminum alloy to steel by friction stir welding", *Journal of Materials Processing Technology*, Vol. 178 No. 1, pp. 342–349.
- [2] Wan, L. and Huang, Y. (2018), "Friction stir welding of dissimilar aluminum alloys and steels: a review", *The International Journal of Advanced Manufacturing Technology*, Vol. 99 No. 5, pp. 1781–1811.
- [3] Fereiduni, E., Movahedi, M. and Kokabi, A.H. (2015), "Aluminum/steel joints made by an alternative friction stir spot welding process", *Journal of Materials Processing Technology*, Vol. 224, pp. 1–10.
- [4] Leitao, C., Arruti, E., Aldanondo, E. and Rodrigues, D.M. (2016), "Aluminium-steel lap joining by multipass friction stir welding", *Materials & Design*, Vol. 106, pp. 153–160.
- [5] Pourali, M., Abdollah-zadeh, A., Saeid, T. and Kargar, F. (2017), "Influence of welding parameters on intermetallic compounds formation in dissimilar steel/aluminum friction stir welds", *Journal of Alloys and Compounds*, Vol. 715, pp. 1–8.
- [6] Chen, K., Liu, X. and Ni, J. (2017), "Keyhole refilled friction stir spot welding of aluminum alloy to advanced high strength steel", *Journal of Materials Processing Technology*, Vol. 249, pp. 452–462.
- [7] Hsieh, M.-J., Lee, R.-T. and Chiou, Y.-C. (2017), "Friction stir spot fusion welding of low-carbon steel to aluminum alloy", *Journal of Materials Processing Technology*, Vol. 240, pp. 118–125.
- [8] Helal, Y., Boumerzoug, Z. and Fellah, L. (2019), "Microstructural evolution and mechanical properties of dissimilar friction stir lap welding aluminum alloy 6061-T6 to ultra-low carbon steel.", *Energy Procedia*, Vol. 157, pp. 208–215.
- [9] Jamshidi aval, H. and Loureiro, A. (2019), "Effect of reverse dual rotation process on properties of friction stir welding of AA7075 to AISI304", *Transactions of Nonferrous Metals Society of China*, Vol. 29 No. 5, pp. 964–975.
- [10] Wang, T., Sidhar, H., Mishra, R.S., Hovanski, Y., Upadhyay, P. and Carlson, B. (2019), "Evaluation of intermetallic compound layer at aluminum/steel interface joined by friction stir scribe technology", *Materials & Design*, Vol. 174, p. 107795.
- [11] Anaman, S.Y., Cho, H.-H., Das, H., Lee, J.-S. and Hong, S.-T. (2019), "Microstructure and mechanical/electrochemical properties of friction stir butt-welded joint of dissimilar aluminum and steel alloys", *Materials Characterization*, Vol. 154, pp. 67–79.
- [12] Shen, Z., Ding, Y., Chen, J., Amirkhiz, B.S., Wen, J.Z., Fu, L. and Gerlich, A.P. (2019), "Interfacial bonding mechanism in Al/coated steel dissimilar refill friction stir spot welds", *Journal of Materials Science & Technology*, Vol. 35 No. 6, pp. 1027–1038.
- [13] Cai, W., Wang, P.C. and Yang, W. (2005), "Assembly dimensional prediction for self-piercing riveted aluminum panels", *International Journal of Machine Tools and Manufacture*, Vol. 45 No. 6, pp. 695–704.
- [14] Abe, Y., Kato, T. and Mori, K. (2006), "Joinability of aluminium alloy and mild steel sheets by self-piercing rivet", *Journal of Materials Processing Technology*, Vol. 177 No. 1, pp. 417–421.
- [15] Abe, Y., Kato, T. and Mori, K. (2009), "Self-piercing riveting of high tensile strength steel and aluminium alloy sheets using conventional rivet and die", *Journal of Materials Processing Technology*, Vol. 209 No. 8, pp. 3914–3922.
- [16] Lazarevic, S., Miller, S.F., Li, J. and Carlson, B.E. (2013), "Experimental analysis of friction stir forming for dissimilar material joining application", *Journal of Manufacturing Processes*, Vol. 15 No. 4, pp. 616–624.
- [17] Evans, W.T., Gibson, B.T., Reynolds, J.T., Strauss, A.M. and Cook, G.E. (2015), "Friction Stir Extrusion: A new process for joining dissimilar materials", *Manufacturing Letters*, Vol. 5, pp. 25–28.

- [18] Huang, Y., Wang, J., Wan, L., Meng, X., Liu, H. and Li, H. (2016), "Self-riveting friction stir lap welding of aluminum alloy to steel", *Materials Letters*, Vol. 185, pp. 181–184.
- [19] Huang, Y., Huang, T., Wan, L., Meng, X. and Zhou, L. (2019), "Material flow and mechanical properties of aluminum-to-steel self-riveting friction stir lap joints", *Journal of Materials Processing Technology*, Vol. 263, pp. 129–137.
- [20] Hussein, S.K., Abdullah, I.T. and Hussein, A.K. (2019), "Spot lap joining of AA5052 to AISI 1006 by aluminium extrusion via friction forming technique", *Multidiscipline Modeling in Materials and Structures*, Vol. 15 No. 6, pp. 1337–1351.
- [21] Destefani, J.D. (1992), "Properties and Selection: Nonferrous alloys and special-purpose materials", *ASM Handbook*, ASM International, USA, Vol. 2, pp. 1–3470.
- [22] Abdullah, I.T. and Hussein, S.K. (2019), "Shear strength and temperature distribution model of friction spot lap joint of high-density polyethylene with aluminum alloy 7075", *International Journal of Structural Integrity*, Vol. 10 No. 4, pp. 469–483.
- [23] Joe Alex, A., Vaira Vignesh, R., Padmanaban, R. and Govindaraju, M. (2020), "Effect of heat treatment on the mechanical and wear behavior of friction stir processed AA5052 alloy", *Materials Today: Proceedings*, Vol. 22, pp. 3340–3346.
- [24] Zareie, O., Mousavizade, S.M., Ezatpour, H.R., Zareie, H. and Farmanbar, N. (2020), "Effect of plunging depth and dwelling time on microstructure and mechanical properties of 6061 aluminum alloy welded by protrusion friction stir spot welding", *Welding in the World*, available at:<https://doi.org/10.1007/s40194-020-00884-5>.
- [25] Abdullah, I.T. and Hussein, S.K. (2018), "Improving the joint strength of the friction stir spot welding of carbon steel and copper using the design of experiments method", *Multidiscipline Modeling in Materials and Structures*, Vol. 14 No. 5, pp. 908–922.